Journal of Nuclear Materials 386–388 (2009) 210–213

Contents lists available at ScienceDirect

Journal of Nuclear Materials

journal homepage: www.elsevier.com/locate/jnucmat

Characterization of deformation structure in ion-irradiated stainless steels

Terumitsu Miura [a,*], Katsuhiko Fujii [a], Koji Fukuya [a], Yoshifumi Ito [b]

[a] Institute of Nuclear Safety System, Incorporated, Fukui, Japan
[b] The Wakasa Wan Energy Research Center, Fukui, Japan

A B S T R A C T

The effects of strain rate and type of stainless steels on the deformation behavior of irradiated stainless steels were investigated. Type 316 and 304 stainless steels irradiated with 200 keV He^+ ions up to 20 dpa at 300 °C were deformed at 10^{-4} and 10^{-7}/s at 300 °C. The deformation changed from uniform dislocation tangling to dislocation channeling and twinning, and slip step spacing widened due to prevention of dislocation gliding by dislocation loops and cavities. The deformation mode was the same in both stainless steels deformed at both strain rates. The loop and cavity density in type 304 stainless steel was smaller than that in type 316 stainless steel. However, dislocation gliding was more effectively prevented in the case of faster deformation and in type 304 stainless steel when dislocation loops were the dominant microstructure. The difference became small at higher doses when cavities were the dominant microstructure.

1. Introduction

Irradiation assisted stress corrosion cracking (IASCC) is a problem for stainless steels used as structural materials of vacuum vessels and in-vessel components of fusion reactor devices [1]. Although the mechanism of IASCC is still unclear, it has recently been suggested that stress concentration at grain boundaries by deformation localization due to irradiation plays an important role in the occurrence and propagation of IASCC in stainless steels [2]. Fukuya et al. have shown that grain boundary separation occurs due to interactions between coarse slips and grain boundaries of stainless steels irradiated in a pressurized water reactor (PWR) [3,4]. Since the grain boundary separation might differ with strain rate and type of stainless steels, it is necessary to investigate the effects of strain rate and type of stainless steels on deformation behavior in order to better understand the role of deformation in intergranular cracking. Deformation behavior has been investigated in ion- and proton-irradiated stainless steels because irradiation conditions are limited for neutron irradiation and it is difficult to perform a number of experiments using radioactivated specimens [5–7]. In this study, the effects of strain rate and type of stainless steels on deformation behavior were investigated in ion-irradiated stainless steels deformed at strain rates of 10^{-4} and 10^{-7}/s at 300 °C.

2. Experimental procedure

Solution annealed type 316 and 304 stainless steels (316SS and 304SS) with average grain sizes of 40 and 85 μm, respectively, were used. The chemical compositions are shown in Table 1. Flat tensile specimens with the gage section of 9 × 3 × 1 mm were polished mechanically and electrolytically to remove surface damage. One side of the gage section was irradiated with 200 keV He^+ ions at 300 °C. The damage peak depth and helium deposition peak depth were calculated to be 520 and 600 nm, respectively, using the SRIM-2000 code [8] with the displacement energy of 40 eV. The irradiation was performed to 0.1, 0.5, 1, 2, 4, 20 dpa at a damage rate of 1.7×10^{-3} dpa/s at the damage peak depth. Microstructure analysis for cross-sections of the specimens using a HITACHI HF-3000 transmission electron microscope (TEM) showed that the depth for the highest density of irradiation defects almost corresponded to the calculated damage peak depth. In this paper, the dose of the specimen was expressed as the dpa value of the damage peak depth.

Hardness was measured using the nano-indentation technique. The indentation depth was set to 150 nm to measure average microhardness of the region from the surface to a depth of about 600 nm. The average dose in this region was about half a dose at the damage peak depth. The microstructure at the damage peak depth was analyzed using a TEM. The TEM samples were prepared by the focused ion beam (FIB) technique to take the damage peak depth into a thin foil with thickness of less than 100 nm. The specimens were tensiled at strain rates of 10^{-4} and 10^{-7}/s to 2% plastic strain at 300 °C in air and pure Ar gas. The angle of slip steps to the

* Corresponding author.
E-mail address: miura@inss.co.jp (T. Miura).

0022-3115/$ - see front matter © 2008 Elsevier B.V. All rights reserved.
doi:10.1016/j.jnucmat.2008.12.093

Table 1
Chemical compositions (wt.%).

	C	Si	Mn	P	S	Ni	Cr	Mo	Fe
316SS	0.048	0.44	1.42	0.024	0.0005	11.05	16.47	2.08	Balance
304SS	0.040	0.31	1.59	0.031	0.001	9.21	18.34	0.37	Balance

tensile axis and average slip step spacing were measured for coarse slip steps in 100 grains on the surface of each tensiled specimen using an optical microscope. Near-surface deformation microstructure was observed by TEM for samples taken from grains where the slip step angle was almost perpendicular to the tensile axis by the FIB processing.

3. Results and discussion

Fig. 1 shows the hardness of the damage region in 316SS and 304SS. The hardness of 316SS increased at 2 dpa and then saturated at higher doses as the irradiation dose increased. The hardness of 304SS was almost the same as that of 316SS in unirradiated condition and increased at 4 dpa and then saturated at 20 dpa as the irradiation dose increased. The increase in hardness of 304SS was smaller than that of 316SS.

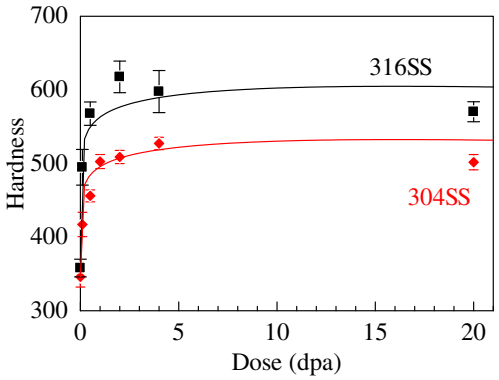

Fig. 1. Hardness of the damage region.

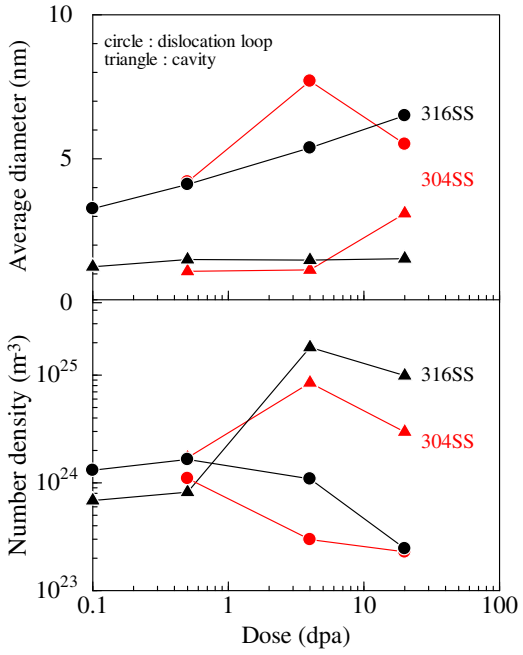

Fig. 2. Average diameter and number density of dislocation loops and cavities at the damage peak depth.

TEM observations revealed that the damage structure consisted of dislocation loops and cavities. Fig. 2 shows the average diameter and number density of dislocation loops and cavities at the damage peak depth in 316SS and 304SS. The loop size increased and cavity size remained almost the same in 316SS as the irradiation dose increased. The loop density decreased at 0.5 dpa whereas the cavity density increased at 4 dpa and decreased at 20 dpa in 316SS. This trend indicates that the dominant defect changed from dislocation loops to cavities at 4 dpa. Although the change of the diameter and density of dislocation loops and cavities in 304SS with the irradiation dose were similar to those in 316SS, the densities of dislocation loops and cavities were rather smaller for 304SS.

Fig. 3 shows the relationship between measured increase in hardness and increase in shear strength calculated by the following equations:

$$\Delta\tau = \sqrt{(\Delta\tau_l)^2 + (\Delta\tau_c)^2}, \tag{1}$$

$$\Delta\tau_{l,c} = \alpha_{l,c}\mu b\sqrt{N_{l,c}d_{l,c}}, \tag{2}$$

where $\Delta\tau$ is the increase in shear strength due to the obstacles of size d, number density N and hardening coefficient α, μ is the shear modulus (64 GPa), b is the size of Burgers vector (0.255 nm); l and c means dislocation loop and cavity, respectively. The hardening coefficient was assumed to be 0.4 and 0.2 for dislocation loop and cavity, respectively. Taylor factor was not used in this calculation because the hardness was measured in near-surface region in a grain. The increase in hardness was almost proportional to the calculated increase in shear strength. The hardening of the damage region was well explained by microstructural data at the damage peak depth. This result indicates that the change of increase in shear strength at the damage peak depth with the irradiation dose was similar to that of the average increase in shear strength in the damage region which would correlate with the increase in hardness, considering the fact that the average dose in the damage region was about half a dose at the damage peak depth.

Fig. 4 shows the distributions of angle of slip steps in 316SS deformed at a strain rate of 10^{-4}/s together with the normalized average shear stress on slip planes calculated without considering

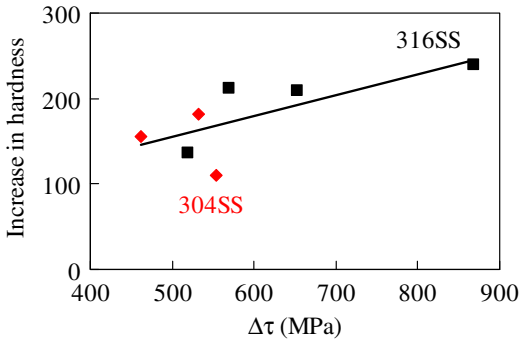

Fig. 3. Relationship between measured increase in hardness and calculated increase in shear strength due to dislocation loops and cavities at the damage peak depth.

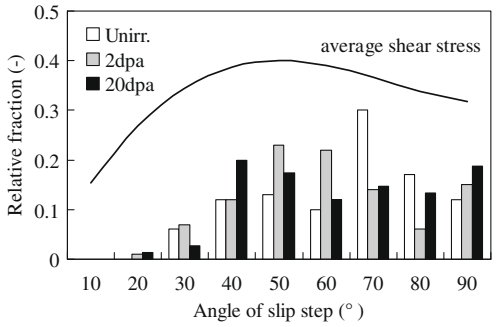

Fig. 4. Angle of slip steps to the tensile axis in 316SS deformed at a strain rate of 10^{-4}/s.

stress component generated from inter-grain interactions. The distributions showed the same trend as the normalized average shear stress. The angle of slip steps in 316SS and 304SS deformed at 10^{-7}/s also showed the same trend. This indicates that the slip steps observed in this study were formed by shear slip.

Fig. 5 shows the average slip step spacing in 316SS and 304SS deformed at strain rates of 10^{-4} and 10^{-7}/s. The spacing increased and then saturated at higher doses as the irradiation dose increased. In 316SS deformed at 10^{-4} and 10^{-7}/s, the spacing was narrower in unirradiated condition, but increased more rapidly as the irradiation dose increased for faster deformation. The difference in the spacing by strain rate became small at higher doses. In 316SS and 304SS deformed at 10^{-7}/s, the spacing in unirradiated 316SS and 304SS were almost the same whereas the spacing increased at a lower dose for 304SS.

Fig. 6 shows cross-sectional TEM images of the microstructure with slip steps in 316SS in unirradiated and 0.5 and 20 dpa conditions after deformation at 10^{-4}/s. Note that the regions of black contrast in the surface region of about 30 nm were damages introduced during the FIB process. The deformation microstructure changed with irradiation dose in the same manner in 316SS and 304SS. Dislocation tangles and dislocation arrays were observed in unirradiated and 0.1 dpa conditions. At doses higher than 0.5 dpa, all slips from the matrix penetrated the damage region containing dislocation loops and cavities as dislocation channels. Some of the slips were blocked in the damage region whereas other slips penetrated through the damage region and formed coarse surface slip steps. Thus, the slip step spacing increased due to a decrease of slips penetrating the damage region. The increase of slip step spacing means that the deformation was more localized in each channel. At 4 and 20 dpa, twins were formed within dislocation channels near the damage peak depth. He bubbles cannot be swept by glide dislocations and become obstacles for dislocation

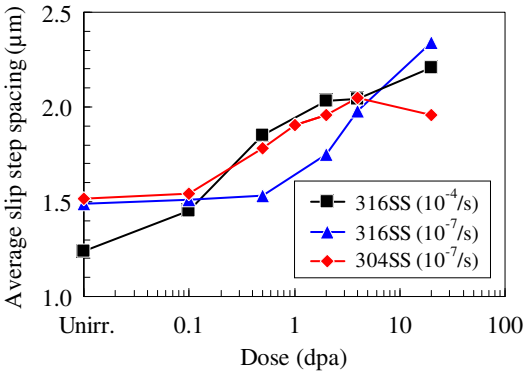

Fig. 5. Averaged slip step spacing deformed at strain rates of 10^{-4}/s and 10^{-7}/s.

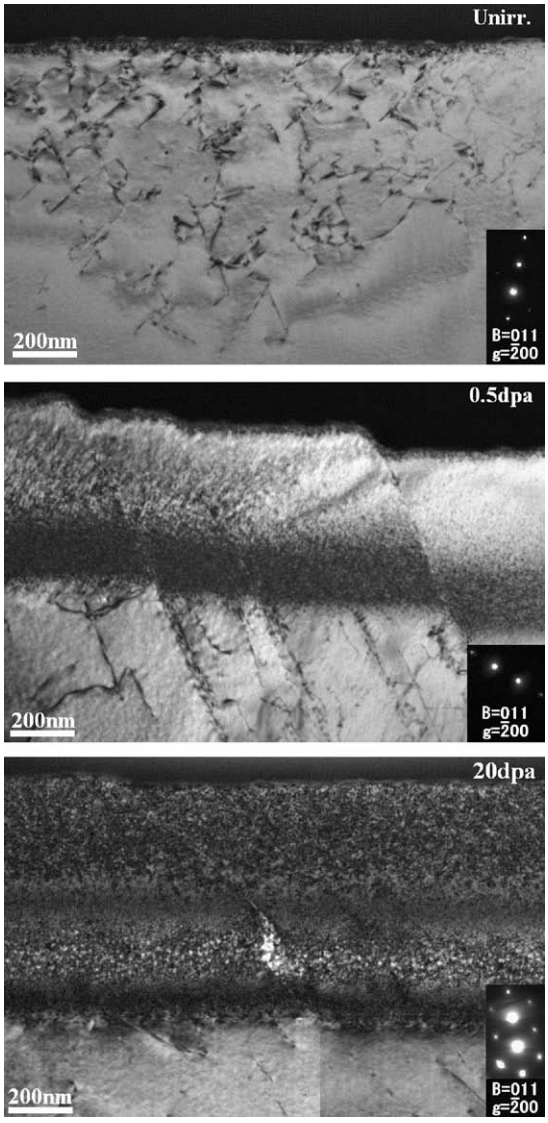

Fig. 6. Microstructure of 316SS deformed at a strain rate of 10^{-4}/s.

motions [7]. Therefore, twinning, which requires a high stress for nucleation, additionally occurred with deformation in the damage region. At the highest dose of 20 dpa, slips penetrated changing slip planes (cross-slips) near the helium deposition peak depth where large He bubbles with a diameter of 30 nm developed. It should be noted that the microstructure at 20 dpa was considerably different from that at 4 dpa due to the large He bubbles.

Although the number densities of dislocation loops and cavities in 304SS were rather smaller than those in 316SS, the slip step spacing increased at a lower dose for 304SS. This is likely due to a difference in stacking fault energy (SFE) of both stainless steels. The SFE of the present 316SS and 304SS were estimated to be 51 and 26 mJ/m^2, respectively [9]. A dislocation extends to two partial dislocations in the face-centered cubic crystal. The width of extended dislocations in 304SS is about twice that in 316SS because the width of extended dislocations is inversely proportional to SFE. Although dislocations can pass irradiation induced defects by cross-slips or climb motions, extended dislocations must constrict before changing slip plane or climbing. The possibility that dislocations pass defects by cross-slips or climb motions decreases for wider extended dislocations because more energy is needed to constrict wider extended dislocations. Therefore, it is likely that

dislocation gliding in 304SS was more effectively prevented by the damage structure compared to that in 316SS and the slip step spacing became wider in 304SS by irradiation.

The slip step spacing in 304SS was wider than that in 316SS at doses from 0.5 to 4 dpa, whereas the hardening of the damage region was smaller for 304SS. This is probably due to the fact that slips started out of the damage region in tensile tests whereas slips occurred within the damage region in hardness measurement.

4. Conclusion

Ion-irradiated 316SS and 304SS were deformed at 10^{-4} and 10^{-7}/s at 300 °C to investigate the effects of strain rate and type of stainless steels on the deformation behavior of irradiated stainless steels. The following results were obtained.

1. The deformation mode in the damage region changed to dislocation gliding restricted to dislocation channels and the slip step spacing at the surface increased with the development of damage structure at doses where dislocation loops were dominant. When cavities were the dominant microstructure at higher doses, twinning occurred additionally in channels near the damage peak depth and cross-slips were pronounced near the helium deposition peak depth.
2. Slip penetration in the damage region was more effectively prevented in the case of faster deformation. The influence of strain rate became small at higher doses when cavities were the dominant microstructure.
3. Dislocation gliding was more effectively prevented when dislocation loops were the dominant microstructure in 304SS compared to 316SS, probably due to lower SFE in 304SS.

References

[1] Y. Miwa, T. Tsukada, S. Jitsukawa, J. Nucl. Mater. 367–370 (2007) 1175.
[2] G.S. Was, Proceedings of 11th International Conference on Environmental Degradation of Materials in Nuclear Power Systems – Water Reactors, ANS (2003) 965.
[3] K. Fukuya, K. Fujii, Y. Kitsunai, Proceedings of 12th International Conference on Environmental Degradation of Materials in Nuclear Power Systems – Water Reactors, TMS (2005) 389.
[4] H. Nishioka, K. Fukuya, K. Fujii, Y. Kitsunai, J. Nucl. Sci. Technol. 45 (2008) 274.
[5] Z. Jiao, J.T. Busby, G.S. Was, J. Nucl. Mater. 361 (2007) 218.
[6] J.I. Cole, S.M. Bruemmer, J. Nucl. Mater. 225 (1995) 53.
[7] T.S. Byun, E.H. Lee, J.D. Hunn, J. Nucl. Mater. 321 (2003) 29.
[8] J.F. Ziegler, J.P. Biersack, U. Littmark, The Stopping and Range of Ions in Solids, Pergamon, New York, 1985.
[9] R.E. Schramm, R.P. Reed, Metall. Trans. A 6A (1975) 1345.